

# Liquid phase epitaxial growth of Fe-doped semi-insulating InGaAsP lattice matched to InP over the entire composition range

著者	中嶋 一雄
journal or publication title	Applied Physics Letters
volume	53
number	7
page range	574-576
year	1988
URL	<a href="http://hdl.handle.net/10097/46959">http://hdl.handle.net/10097/46959</a>

doi: 10.1063/1.99861

# Liquid phase epitaxial growth of Fe-doped semi-insulating InGaAsP lattice matched to InP over the entire composition range

M. Kondo, M. Sugawara, T. Tanahashi, S. Isozumi, and K. Nakajima  
*Fujitsu Laboratories, Atsugi, 10-1 Morinosato-Wakamiya, Atsugi 243-01, Japan*

(Received 14 March 1988; accepted for publication 14 June 1988)

Fe-doped semi-insulating  $\text{In}_{1-x}\text{Ga}_x\text{As}_y\text{P}_{1-y}$  ( $0 < y < 1$ ,  $y = 2.2x$ ) epitaxial layers lattice matched to InP with nearly intrinsic carrier concentrations have been successfully grown over the entire composition range by liquid phase epitaxy. Maximum resistivities as high as  $8 \times 10^7 \Omega \text{ cm}$  for InP,  $2 \times 10^5 \Omega \text{ cm}$  for InGaAsP ( $y = 0.57$ ), and  $2 \times 10^3 \Omega \text{ cm}$  for InGaAs ( $y = 1$ ) have been achieved. The critical growth temperature necessary to obtain semi-insulating layers significantly decreased as the composition was varied from  $y = 0$  to  $y = 1$ . The Fe doping characteristics are well defined by the composition dependence of the Fe distribution coefficient.

High-resistivity (HR) or semi-insulating (SI)  $\text{In}_{1-x}\text{Ga}_x\text{As}_y\text{P}_{1-y}$  epitaxial layers lattice matched to InP ( $0 < y < 1$ ,  $y = 2.2x$ ) have considerable potential to improve the performance of high-speed<sup>1</sup> and optoelectronic devices<sup>2-6</sup>. In particular, the use of SI InP epitaxial layers for current confinement in InGaAsP/InP buried-heterostructure (BH) lasers has been attracting much interest in recent years, since SI InP layers can eliminate both leakage current and parasitic capacitance. It has been demonstrated that such novel BH lasers exhibit low threshold current, high light output power, and, in particular, excellent high-frequency modulation performance.<sup>4-6</sup>

In the InGaAsP system, it has been established that HR InGaAs ( $y = 1$ ) can be grown by liquid phase epitaxy (LPE) using Fe as a dopant.<sup>7-9</sup> However, previous attempts of LPE growth of Fe-, Cr-, and Co-doped SI InP have been unsuccessful.<sup>10,11</sup> The difficulty of this approach has been attributed to the formation of precipitates between the phosphorus and the transition metal in growth solutions.<sup>11</sup> The first epitaxial growth of SI InP was accomplished by metalorganic vapor phase epitaxy and Fe doping.<sup>12</sup>

Recently, we demonstrated that Fe-doped SI InP layers can be obtained by LPE at growth temperatures above  $850^\circ\text{C}$ .<sup>13</sup> Researchers also reported that LPE-grown Fe-doped SI InP layers are free from Fe-P precipitates.<sup>14</sup>

Although LPE is the most common method used to fabricate optoelectronic devices like BH lasers, the growth temperature required to obtain Fe-doped SI InP is too high for device applications. Therefore, the growth temperature should be decreased as much as possible. In this study, we extended Fe doping of the InGaAsP system over the entire range of composition, and attempted the low-temperature growth of SI layers in the quaternary region. We demonstrate that Fe-doped SI InGaAsP layers can be grown over the entire range of composition by LPE. We also show that the growth temperature necessary to obtain SI layers can be significantly reduced by changing the composition from  $y = 0$  to  $y = 1$ . The crucial parameters that determine the Fe doping behavior are also clarified.

The epitaxial layers were grown on (100) oriented Sn-doped  $n^+$ -InP or Fe-doped SI InP substrates using a graph-

ite sliding boat system. The materials used were commercially available 99.99999% pure indium, single-crystal GaAs and InP, polycrystal InAs, and 99.99% pure Fe powder. As reported by the researchers in Ref. 15, Fe introduces a deep acceptor state at almost the middle of the forbidden energy band of the InGaAsP system over the entire composition.

Fe doping was performed for three compositions of the InGaAsP system lattice matched to InP: InP,  $\text{In}_{0.74}\text{Ga}_{0.26}\text{As}_{0.57}\text{P}_{0.43}$ , and  $\text{In}_{0.53}\text{Ga}_{0.47}\text{As}$ . The growth temperature was varied between  $650$  and  $900^\circ\text{C}$ . To eliminate thermal damage to InP substrates and epitaxial layers at high temperature, an InP wafer was faced to an InP substrate until the growth started, then another InP wafer was faced to an epitaxial layer immediately after the growth. Fe was added to the growth solutions between 0.004 and 2.0 weight percent (wt. %). To minimize the formation of the precipitates like Fe-As or Fe-P, the temperature of the furnace was raised quickly to about  $15^\circ\text{C}$  above the growth temperature, and then cooled down. Typically, the growth solution was above the growth temperature for 10–15 min before the growth began.

For reproducible growth of SI crystals, low background carrier concentration is the most critical factor. In this study, high-purity epitaxial layers with low background carrier concentrations were reproducibly obtained over the entire composition without any purification procedures for the growth solutions. The background carrier concentrations of undoped layers were between  $6 \times 10^{14}$  and  $1 \times 10^{15} \text{ cm}^{-3}$ . These values were almost independent of growth temperatures between  $650$  and  $900^\circ\text{C}$ .

The resistivities were measured using van der Pauw samples. When the resistivity exceeded the mid  $10^5 \Omega \text{ cm}$  range, the resistivity was calculated from the current-voltage ( $I$ - $V$ ) characteristics of  $n^+$ -SI- $n^+$  diodes. The fabrication procedures of the diodes are described in Ref. 14.

Secondary ion mass spectroscopy (SIMS) analysis was performed to estimate the Fe concentrations in the epitaxial layers. Quantitative analysis for Fe was based on a relative sensitivity factor determined from an Fe ion implanted InP reference for the InP layers, or an Fe ion implanted GaAs reference for the InGaAs ( $y = 1$ ) layers. For the quaternary

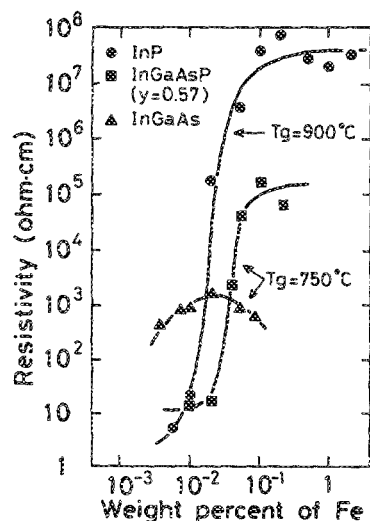


FIG. 1. Resistivity of Fe-doped InP grown at 900 °C, Fe-doped InGaAsP ( $y = 0.57$ ) and InGaAs ( $y = 1$ ) grown at 750 °C, as a function of the weight percent of Fe in the growth solution.

layers, the relative sensitivity factor was corrected according to the arsenic alloy composition ( $y$ ). The accuracy of the quantitative analysis was within a factor of 2. The Fe background concentrations for the analysis were approximately  $1 \times 10^{15} \text{ cm}^{-3}$ . The Fe concentrations of LPE-grown Fe-doped layers estimated by SIMS analysis were close to those obtained from the  $J$ - $V$  characteristics of  $n^+ \text{-SI-} n^+$  diodes and deep level transient spectroscopy.<sup>14</sup>

Figure 1 shows the resistivity of Fe-doped InP grown at 900 °C, Fe-doped InGaAsP ( $y = 0.57$ ) and InGaAs ( $y = 1$ ) grown at 750 °C versus the weight percent of Fe ( $W_{\text{Fe}}$ ) in the growth solution. High-resistivity or semi-insulating layers were successfully grown over the entire composition. The maximum resistivities achieved so far are  $8 \times 10^7 \Omega \text{ cm}$  for  $y = 0$ ,  $2 \times 10^5 \Omega \text{ cm}$  for  $y = 0.57$ , and  $2 \times 10^3 \Omega \text{ cm}$  for  $y = 1$ . Taking the band-gap energy and the effective masses into account, the resistivities for the intrinsic condition at 300 K were calculated to be  $2 \times 10^8 \Omega \text{ cm}$  for  $y = 0$ ,  $1 \times 10^5 \Omega \text{ cm}$  for  $y = 0.57$ , and  $1 \times 10^3 \Omega \text{ cm}$  for  $y = 1$ .<sup>16</sup> The maximum resistivities of Fe-doped layers obtained in our experiments are close to those for the intrinsic condition.

In Fig. 1, the resistivity of each sample increased abruptly

TABLE I. Fe concentration in Fe-doped layers estimated by SIMS analysis. Growth conditions and the resistivity are also shown.

No.	Material	$T_g$ (°C)	$W_{\text{Fe}}$ (wt. %)	$X_{\text{Fe}}^s$ ( $10^{15} \text{ cm}^{-3}$ )	Resistivity ( $\Omega \text{ cm}$ )
171	InP	800	0.10	1.5	6
166	InP	850	0.10	4	$3 \times 10^5$
212	InP	900	0.010	2	20
207	InP	900	0.10	7	$4 \times 10^7$
232	InP	900	1.0	8	$5 \times 10^7$
424	InGaAsP ( $y = 0.57$ )	750	0.10	2	$2 \times 10^5$
606	InGaAsP ( $y = 0.57$ )	780	0.10	4	$8 \times 10^4$
489	InGaAs ( $y = 1$ )	650	0.10	4	...
363	InGaAs ( $y = 1$ )	750	0.10	30	$7 \times 10^2$

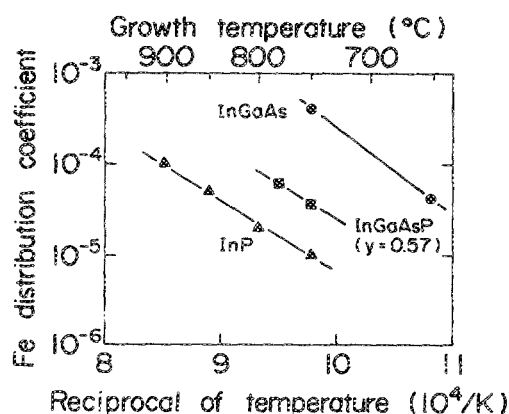


FIG. 2. Fe distribution coefficient for InP, InGaAsP ( $y = 0.57$ ), and InGaAs ( $y = 1$ ) as a function of the reciprocal of growth temperature. The Fe distribution coefficient was estimated using the result of SIMS analysis shown in Table I.

ly at a critical value of  $W_{\text{Fe}}$ . After the abrupt increase, the resistivity of InP and InGaAsP ( $y = 0.57$ ) became saturated in spite of further increases of  $W_{\text{Fe}}$ . As we pointed out in Ref. 13, the saturation of the resistivities occurs because the Fe concentration dissolved in a growth solution reaches the solubility limit. According to Ref. 11, the Fe solubility in pure indium is 0.12 wt. % at 750 °C and 0.33 wt. % at 900 °C. Both values are in good agreement with  $W_{\text{Fe}}$  at which the resistivities saturate. This result also shows that neither Fe-As nor Fe-P precipitates are formed in the growth solutions. The resistivity curve of Fe-doped InGaAs ( $y = 1$ ) reflects two-type carrier conduction, as is predicted in Ref. 8.

Table I summarizes the Fe concentrations in the doped layers ( $X_{\text{Fe}}^s$ ) estimated by SIMS analysis, together with the growth conditions and the resistivity of each layer. The Fe concentrations were in the range of low  $10^{15} \text{ cm}^{-3}$  to mid  $10^{16} \text{ cm}^{-3}$  depending on growth conditions, that is, composition, growth temperature, and Fe doping level.

An important point in Fe doping behavior was that there existed a critical growth temperature above which SI layers could be grown. More important, this critical growth temperature significantly decreased as the composition was varied from  $y = 0$  to  $y = 1$ . For example, the critical growth temperature was between 800 and 850 °C for InP.<sup>13</sup> In this experiment, we found that the critical growth temperature decreased to between 700 and 750 °C for  $y = 0.57$ , and below 650 °C for  $y = 1$ .

This behavior can be explained by the composition dependence of the Fe distribution coefficient ( $k_{\text{Fe}}$ ). Figure 2 shows the Fe distribution coefficient for  $y = 0, 0.57$ , and 1 versus the reciprocal of growth temperature. The Fe distribution coefficient was calculated using the results of the SIMS analysis shown in Table I. As seen in Fig. 2, at a specific growth temperature, the Fe distribution coefficient significantly increases as the composition is varied from  $y = 0$  to  $y = 1$ . The value of  $k_{\text{Fe}}$  was calculated to be  $1 \times 10^{-5}$  for  $y = 0$ ,  $4 \times 10^{-5}$  for  $y = 0.57$ , and  $4 \times 10^{-4}$  for  $y = 1$  at  $T_g = 750$  °C. We also found that the Fe distribution coefficient has the same positive dependence on growth temperature over the entire composition.

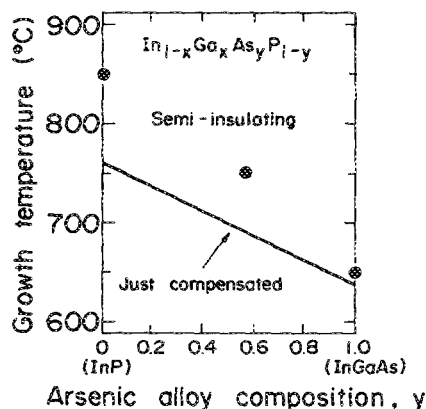


FIG. 3. Growth temperature necessary to obtain SI layers as a function of the composition.

From the results described above, it is shown that Fe doping characteristics of this system can be completely explained in terms of the Fe solubility and the Fe distribution coefficient. By considering behaviors of these two factors, we calculated the critical growth temperature as a function of the composition. The calculation assumed that a SI layer is obtained when an Fe concentration in the epitaxial layer exceeds a background electron concentration of  $1 \times 10^{15} \text{ cm}^{-3}$ . Data for the Fe solubility in indium was taken from Ref. 11.

Figure 3 shows the result of the calculation. At the growth temperature shown by a solid line, epitaxial layers are just compensated, and SI layers are obtained in the region above the line. Solid circles in Fig. 3 represent growth temperatures at which SI layers were obtained in our experiments. The calculation showed that the critical growth temperature decreases from 760 °C for  $y = 0$  to 640 °C for  $y = 1$ . Our results were in good agreement with this calculation.

For applications using SI layers for current blocking in BH lasers, SI quaternary layers are as promising as SI InP layers, if the composition is approximately chosen with respect to an active layer. Therefore, the low-temperature growth of SI layers in the quaternary region is very promising for device applications.

In conclusion, Fe-doped SI InGaAsP layers lattice matched to InP have been successfully grown over the entire composition range. The growth temperature necessary to obtain SI layers could be significantly reduced as the composition was varied from  $y = 0$  to  $y = 1$ . It was found that the Fe doping behavior is due to the high Fe distribution coefficient in the quaternary region.

<sup>1</sup>H. H. Wieder, J. L. Veteran, A. R. Clawson, and D. P. Mullin, *Appl. Phys. Lett.* **43**, 287 (1983).

<sup>2</sup>M. V. Rao and P. K. Bhattacharya, *Electron. Lett.* **20**, 812 (1984).

<sup>3</sup>V. Diadiuk and S. H. Groves, *Appl. Phys. Lett.* **46**, 157 (1985).

<sup>4</sup>N. K. Dutta, J. L. Zilko, T. Cella, D. A. Ackerman, T. M. Shen, and S. G. Napholtz, *Appl. Phys. Lett.* **48**, 1572 (1986).

<sup>5</sup>W. H. Cheng, C. B. Su, K. D. Buehring, J. W. Ure, D. Perrachione, D. Renner, K. L. Hess, and S. W. Zehr, *Appl. Phys. Lett.* **51**, 155 (1987).

<sup>6</sup>T. Sanada, K. Nakai, K. Wakao, M. Kuno, and S. Yamakoshi, *Appl. Phys. Lett.* **51**, 1054 (1987).

<sup>7</sup>A. R. Clawson, D. P. Mullin, and D. I. Elder, *J. Cryst. Growth* **64**, 90 (1983).

<sup>8</sup>S. H. Groves, V. Diadiuk, M. C. Plonko, and D. L. Hovey, *Appl. Phys. Lett.* **46**, 78 (1985).

<sup>9</sup>M. V. Rao and P. K. Bhattacharya, *J. Appl. Phys.* **57**, 333 (1985).

<sup>10</sup>E. A. Rezek, L. M. Zinkiewicz, and H. D. Law, *Appl. Phys. Lett.* **43**, 378 (1983).

<sup>11</sup>R. L. Messham, A. Majerfeld, and K. J. Bachmann, in *Semi-Insulating III-V Materials*, edited by S. M. Ebeid and B. Tuck (Shiva, United Kingdom, 1982), pp. 75-77.

<sup>12</sup>J. A. Long, V. G. Riggs, and W. D. Johnston, Jr., *J. Cryst. Growth* **69**, 10 (1984).

<sup>13</sup>M. Kondo, M. Sugawara, A. Yamaguchi, T. Tanahashi, S. Isozumi, and K. Nakajima, in *Extended Abstracts of the 18th International Conference on Solid State Devices and Materials* (Business Center for Academic Societies Japan, Tokyo, 1986), pp. 627-630.

<sup>14</sup>M. Sugawara, M. Kondo, K. Nakai, A. Yamaguchi, and K. Nakajima, *Appl. Phys. Lett.* **50**, 1432 (1987).

<sup>15</sup>M. Sugawara, M. Kondo, T. Takanohashi, and K. Nakajima, *Appl. Phys. Lett.* **51**, 834 (1987).

<sup>16</sup>Parameters used in the calculation are listed in the appendix of *GaInAsP Alloy Semiconductor*, edited by T. P. Pearsall (Wiley, New York, 1982), pp. 456-457.